Characterizing Mixing in Lithographed Flow Device

Vann Brasher

ChE 499 with Prof. Finlayson, Spring, 2008

I. Introduction

We are seeking a micro fluidic device that allows for the highest quality of mixing, to aid the efficient study and application of small scale fluid samples, reactions, etc. This report explores the quality of mixing in the micro fluidic device shown in figure 1, which appears in a 2001 *Lab on a Chip* article by Peter Hinsmann. A two dimensional geometry was created in Comsol Muliphysics to approximate and analyze the mixing, using laminar flow and convection and diffusion applications. After data was collected on the 2-D model, a three dimensional model was analyzed as well.

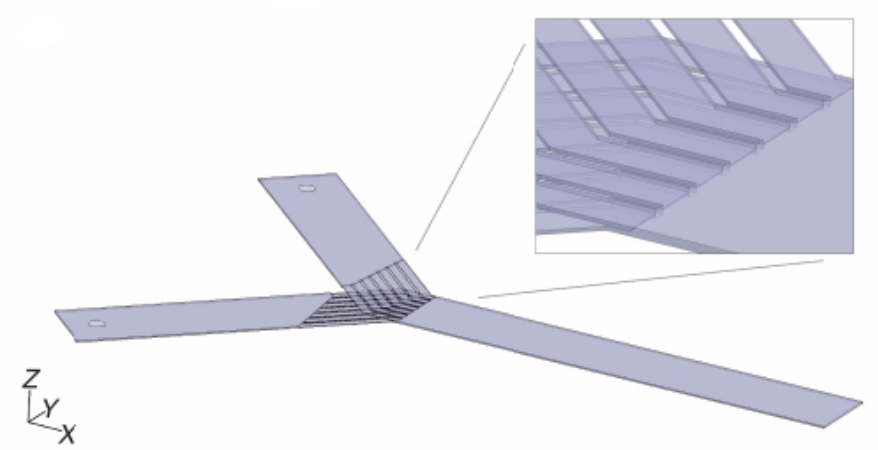

Figure 1: A 3-D picture of the mixing device from Hinsmann's article. This report analyzed a 2-D and 3-D geometry approximation (1).

II. Methods

A two dimensional geometry was created in Comsol Multiphysics software to approximate and qualitatively model the mixing in the device and can be seen in figure 2. The chemical engineering 'incompressible Navier-Stokes' for laminar flow and the chemical engineering 'convection and diffusion' multiphysics options were applied to the geometry.

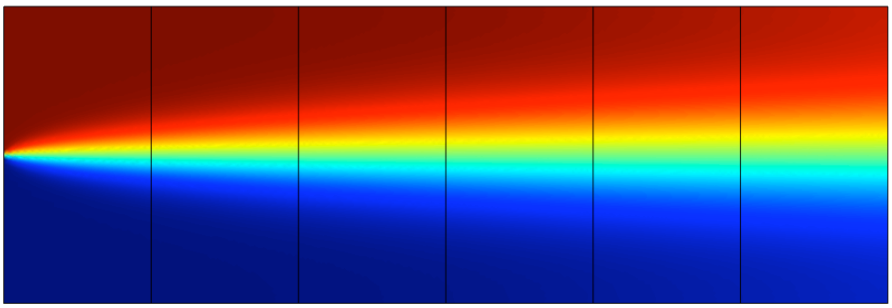

Figure 2: A surface plot of a concentration solution to the 2-D geometry. The dark red is concentration of 1, while dark blue is concentration 0. Colors in between represent concentrations from 0-1 with green being .5. The Peclet number here is 100.

The sub domain settings were set to make use of the non-dimensional forms of the Navier-Stokes and convective diffusion equations shown as equation 1 and 2 below, respectively. The density was set to 1 and eta was set to 1/Re. The Reynolds number was made to be 1, which is a good approximation for the laminar flow of microfluidics. The diffusivity was set at 1/Pe, and the Peclet number was varied in the models to collect different sets of data. The outlet width (x_0) as well as the outlet velocity (v_0) set at one on the model for ease of scaling. Walls were made to be non-slip, the outlet was set at convective flux and the inlet was laminar inflow with a velocity of 1 m/s. The upper half of the inlet was set at a concentration of 1(red) while the lower was set at concentration 0 (blue).

(Eq. 1) $$u' \cdot \nabla' u' = -\nabla' p'' + \frac{1}{\mathrm{Re}} \nabla'^2 u'$$

(Eq. 2) $$u' \cdot \nabla' \cdot c' = \frac{1}{Pe} \cdot \nabla'^2 \cdot c'$$

(2)

The mixing was characterized using five different values: the mixing cup concentration, the concentration variance, the optical mixing cup concentration, the

optical mixing cup concentration variance, and the pressure drop. The pressure drop will be converted from its non-dimensional form to a specific case where the density is 1000 kg/m^3 and the average velocity is .005 m/s. The concentrations provide an average value of concentration at a given length down the mixing chamber, which was generally .5. The variances give a value of how varied the concentration is, at a given length, from the average and provides a quality of mixing measurement. 'Better mixing' would be indicated by a lower variance with an average concentration (c_{mixing_cup}) that indicates good mixing (.5 in our case). The equation for each characterizing value is below. The integrals are taken using boundary integration along the width (w) of the device.

(Eq. 3) $$c_{mixing\_cup} = \frac{\int c \times u dw}{\int u dw}$$

(Eq. 4) $$\text{var}\,iance = \frac{\int (c - c_{mixing\_cup})^2 u dw}{\int u dw}$$

(Eq. 5) $$c_{optical} = \frac{\int c dw}{\int dw}$$

(Eq. 6) $$optical\_\text{var}\,iance = \frac{\int (c - c_{mixing\_cup})^2 dw}{\int dw}$$

(Eq. 7) $$p' = \frac{p}{\rho < v >^2} \quad (2)$$

A picture of the three dimensional case is shown in figure 3. Five channels were constructed on the top and bottom of width .14 with .075 separations, giving an entrance

width of 1. The five channels on top were given a concentration of 1 while the channels on bottom were given a concentration of 0. The mixing chamber has 1x1 entrance area and length of 3. The velocity at the channel inlets was set to 1.5 m/s, giving outlet velocity of the mixing chamber of 1.05 m/s. All other boundary conditions model the 2-D case with interior boundaries set at flux discontinuity. The same equations were used with boundary integration occurring across the area dA instead of the width dw.

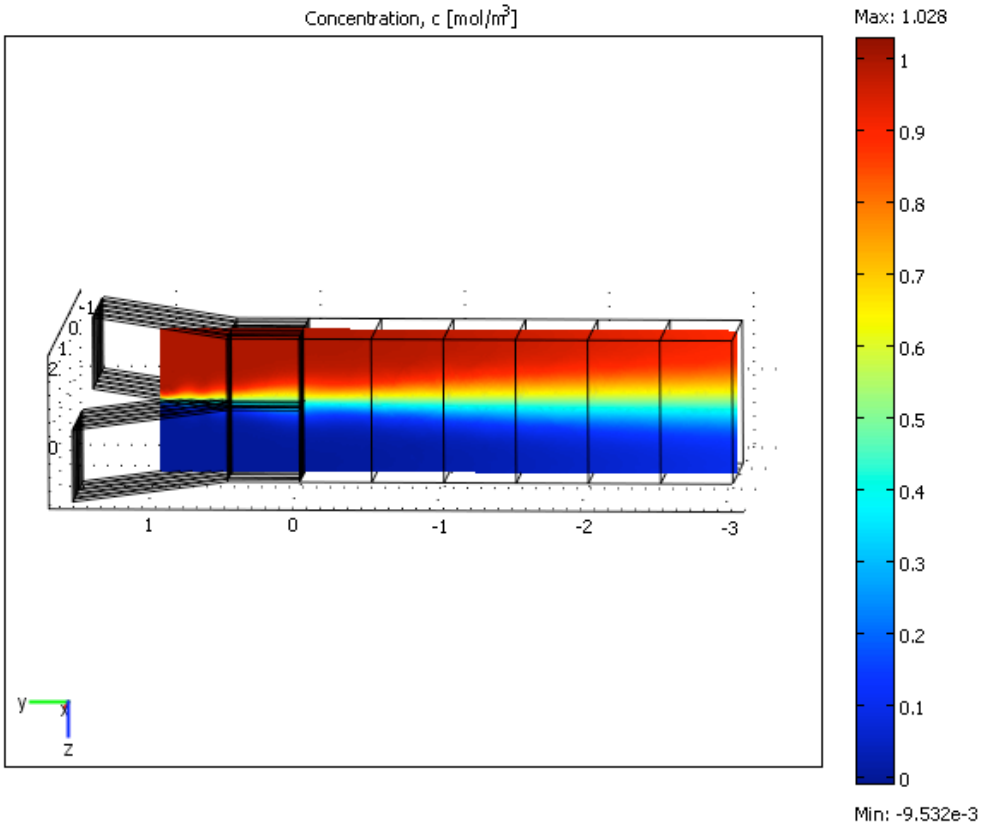

Figure 3: Concentration solution at the centerplane for the 3-D model at Peclet number of 100. Dark red is concentration 1, dark blue is concentration 0, and green is .5.

To decide on the validity and meaning of the results, the mixing data compiled was compared to data on a T-sensor as well as data in Hinsmann's paper, which required an extrusion of the model to dimensionless distance of 25 and Pe=4000.

III. Results

The five characterizing values were calculated at unitless lengths of .5, 1, 1.5, 2, 2.5 and 3 for Peclet numbers of 10, 50, 100, 200, 300, 500, 700, and 1000. The full set of data is given in the appendix. Two-dimensional meshes used for Navier-Stokes solutions contained 5400 coarse elements, which eliminated most waves or spotting on the solution. The mesh was refined specifically in the center of the geometry, after the solution was solved, and the solution was used to resolve for the concentration only. These meshes contained 40,000 elements and up, which removed any spotting or waves from the solution. The variances for each of these concentrations varied with Peclet number and distance and are represented in figure 4. Figure 4 shows all of the mixing cup variance values graphed against x'/Pe, which is the dimensionless distance past the initial mixing point divided by the Peclet number.

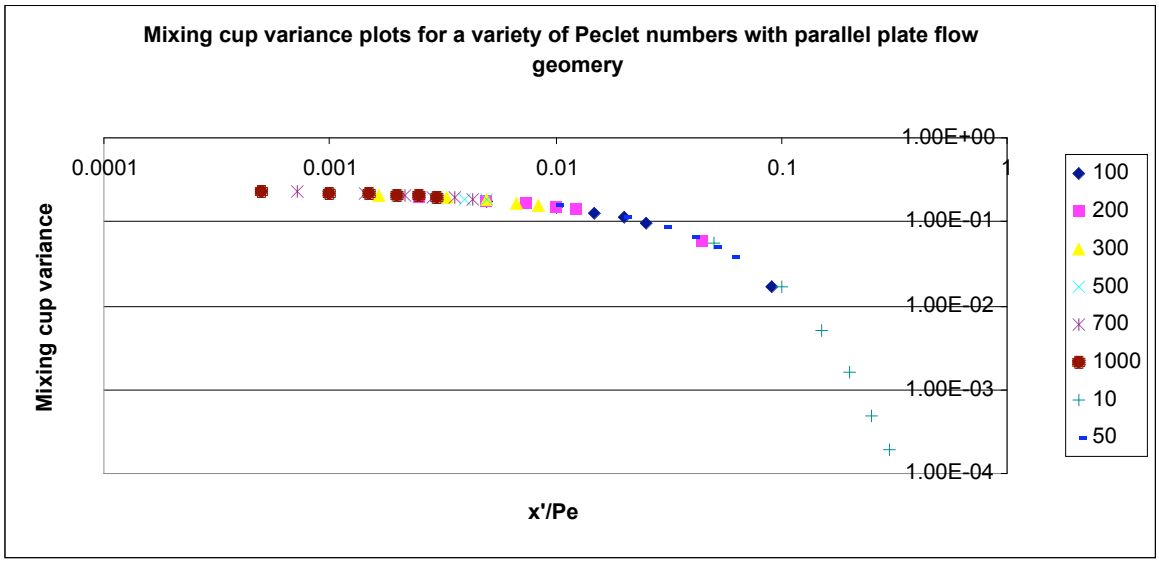

Figure 4: This is the mixing results for the 2-D geometry. All of the data collapses onto one curve.

The 3-D geometry was run with a mesh of 41479 elements. The number of degrees of freedom solved with the Navier-Stokes equation was 190907. For the

convective diffusion equation there were 60753 degrees of freedom solved for. The results for the mixing cup variance of the 3-D model are shown in figure 5. This data collapses onto a single curve. The pressure drop across the mixing chamber is shown in figure 6.

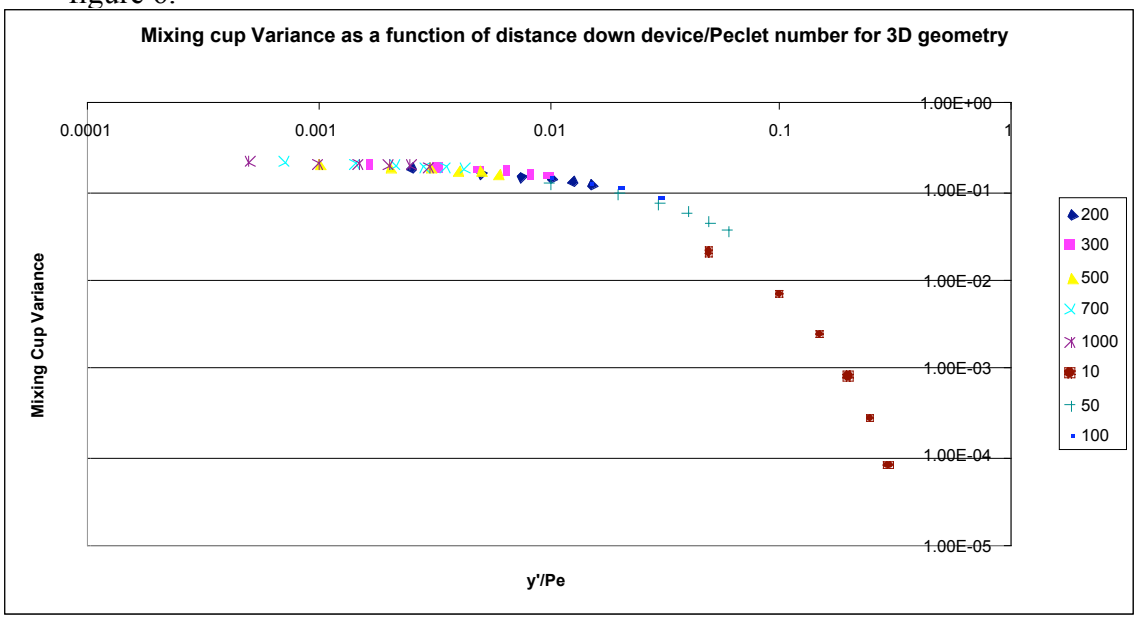

Figure 5: These are the mixing results for the 3-D geometry. The data fit fairly well to one common curve. The mixing cup variance is plotted as a function of the length down the device divided by the Peclet number.

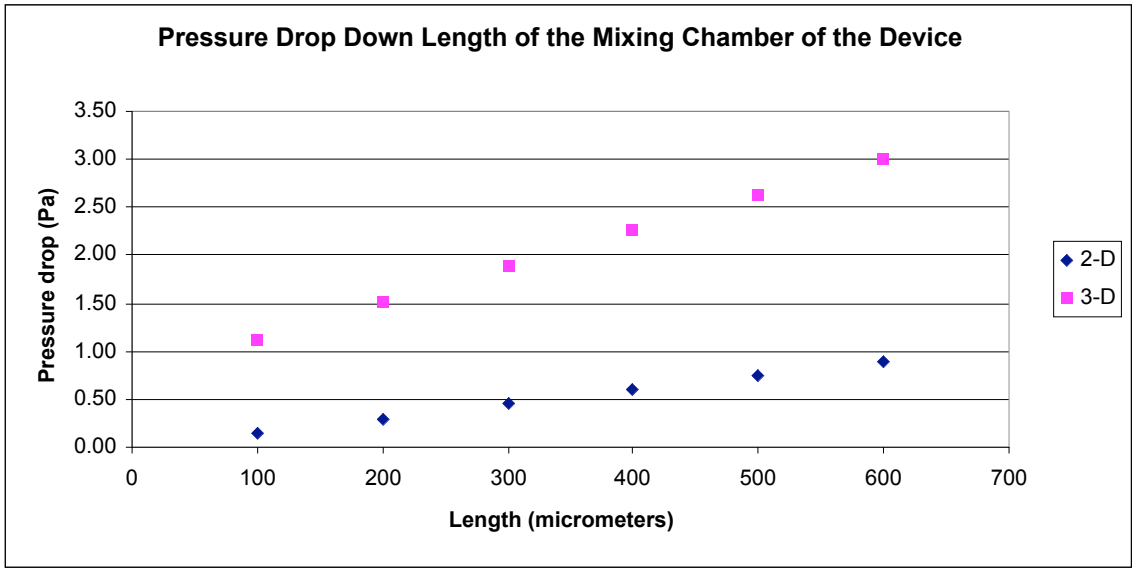

Figure 6: This is the pressure drop down the mixing chamber for both the 2-D and 3-D geometries. Sample calculations can be seen in the appendix. The 3-D case has more pressure drop due to the additional friction from the increased wall area.

The mixing data for the T-sensor is shown in figures 7 and 8. It is qualitatively and quantitatively very similar to the data that was acquired from the model researched. This would indicate similar mixing quality and process. Figure 9 shows Hinsmann's findings of concentrations as a function of thickness for varying lengths down the mixing chamber. Figure 10 has the same axes as figure 9 and is my data at a length corresponding to 0.5mm in Hinsmann's graph. They are similar in shape and number, which provides validity and a check for the model used. The last figure, figure 11, shows both the 2-D and 3-D mixing data on the same curve for comparison. The curves are nearly the same and have no meaningful difference in value.

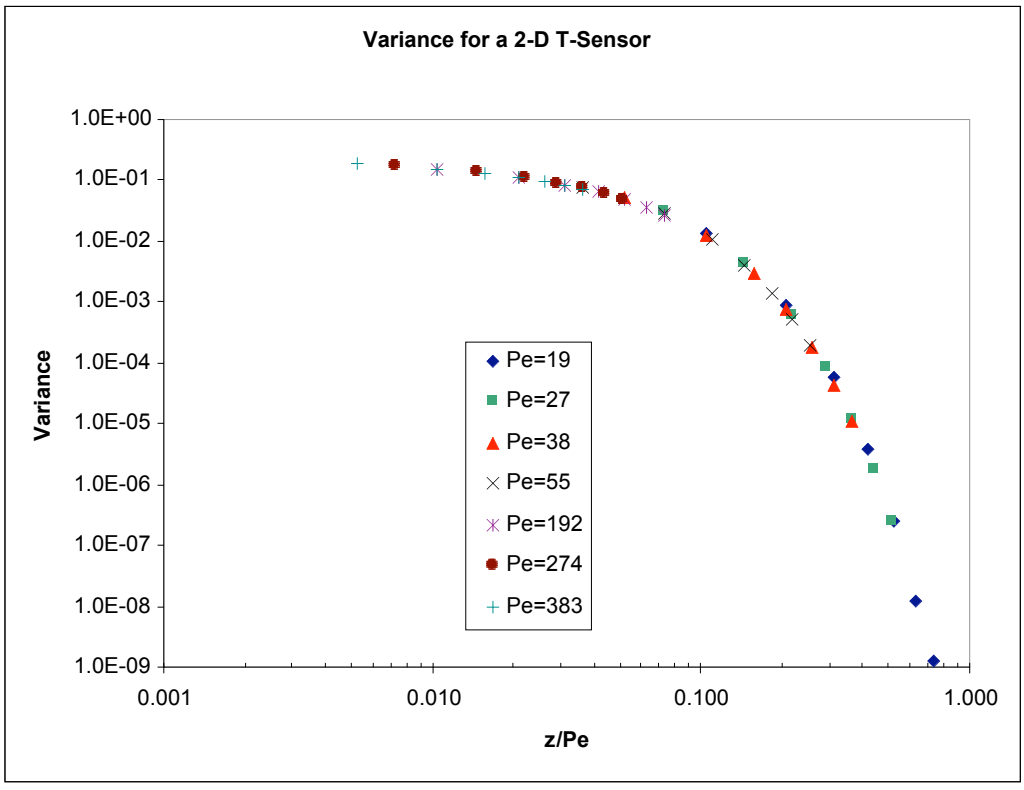

Figure 7: 2-D data for the T-sensor. Provided for comparison (3).

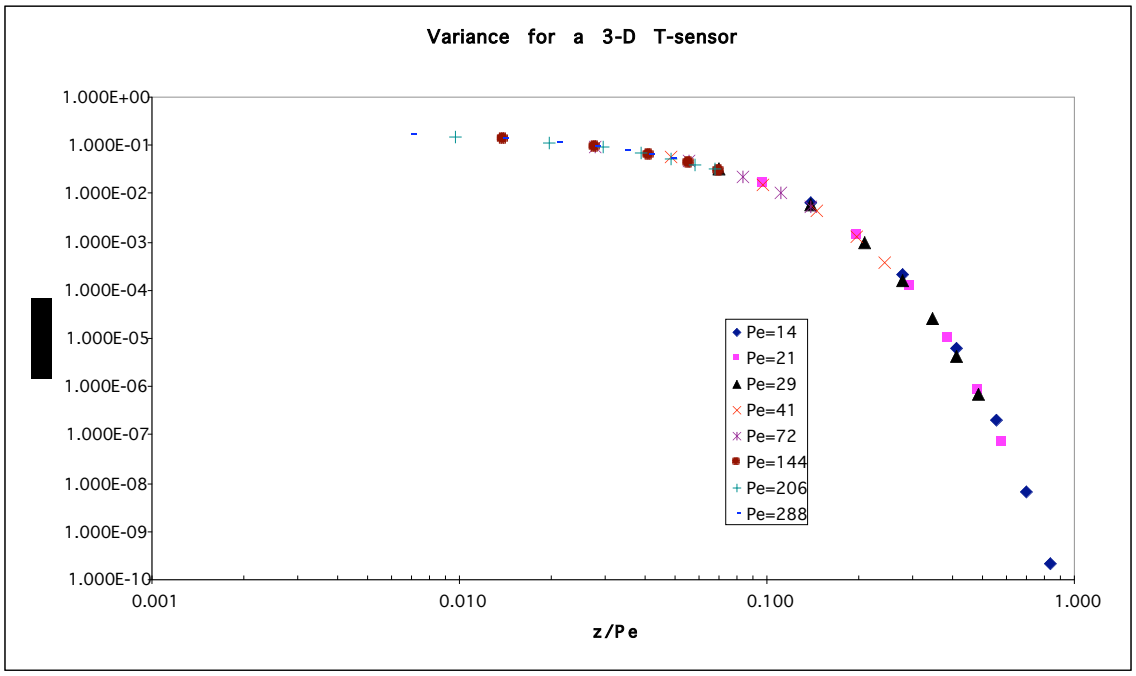

Figure 8: 3-D mixing data for a T-sensor. Provided for comparison (3)

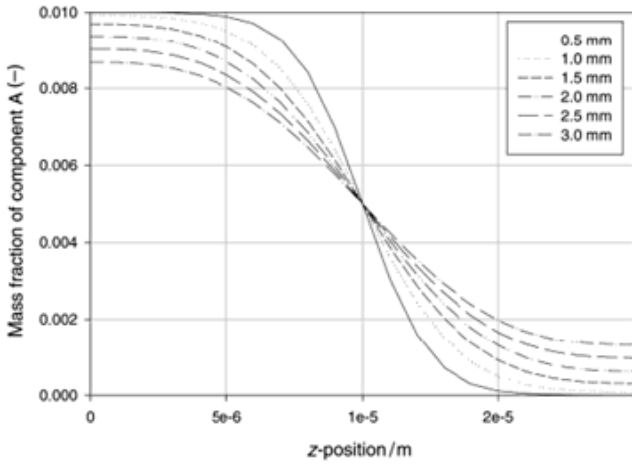

Figure 9: Graph reproduced from Hinsmann's article. This shows concentration as a function of thickness for Various lengths down the mixing chamber (1).

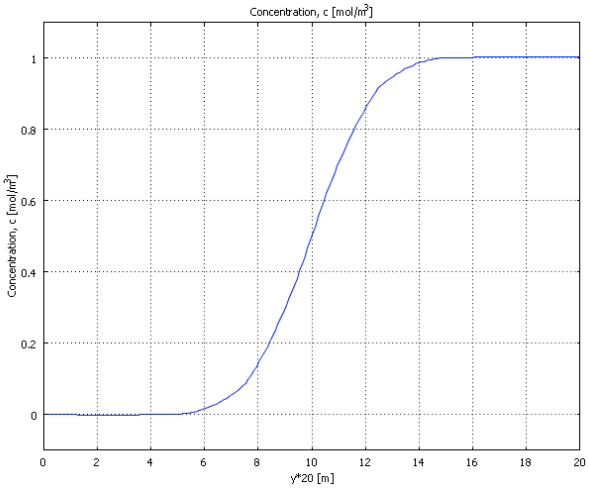

Figure 10: Concentration as a function of thickness for my 2-D geometry. This is at a dimensionless length of 25 and Pe=4000 which corresponds to Hinsmann's curve at .5mm.

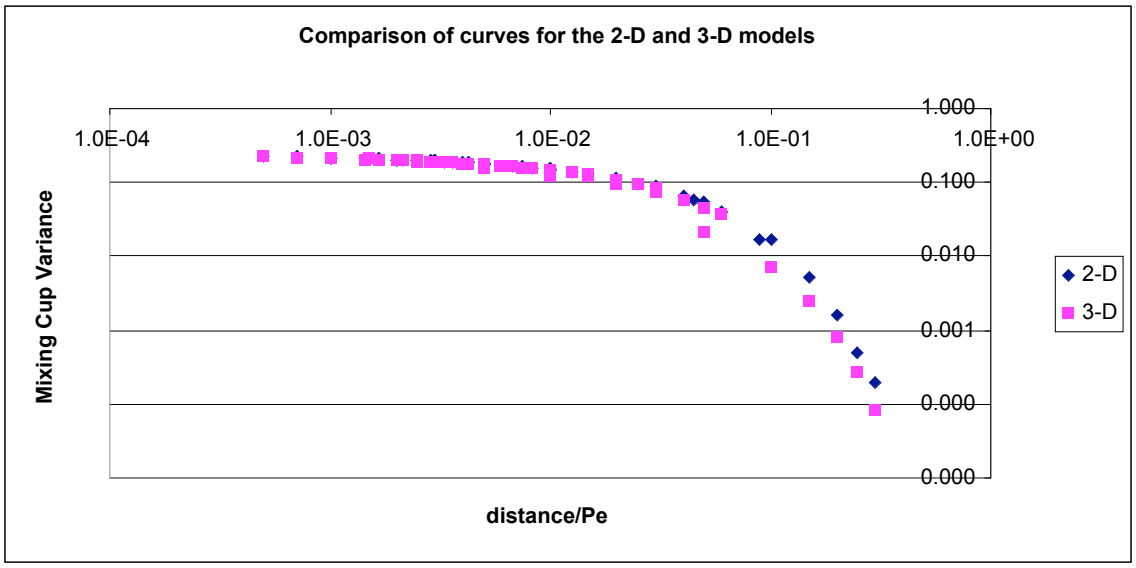

Figure 11: The mixing data for the 2-D and 3-D models overlaid on one another. Any difference in values seen is negligible.

IV. Improvements

This mixing device can be vastly improved. Altered angle of approach and some form of disturbance after the initial mixing along the length of the device should be looked into. Varying the Reynolds number of one or both sides would be an area of further pursuit. A new type of device would be favored on the basis of these results, rather than any improvements on the modeled device of this paper's research.

V. Conclusions

An important result here is that for varying Peclet numbers, the variance collapses onto one curve for z'/Pe, giving a characteristic curve for the device qualitatively similar to a T-sensor. The values for the variance to characterize the mixing are fairly unimpressive, however. The device quantitatively does, at best, as good at mixing as the

T-sensor does. This does not excite the researcher into the outlook of improving mixing with the modeled device. Ultimately the device is a T-sensor only with more parallel entrance flow, limiting the chance for mixing by fluid motion. The 2-D and 3-D model differ by much less than an order of magnitude, as has been shown, so the simple 2-D model is concluded as approximating the mixing in a satisfactory way. No further 3-D modeling is necessary. The mixing cup variance and optical variance differ, but not by an order of magnitude and this leads me to conclude the difference negligible in lab practices.

VI. References

(1) Hinsmann. *Lab on a Chip.* **1** 16 (2001)

(2) Finlayson, Bruce, et. al. *Microinstrumentation Handbook.* Ch. 8.

(3) "Mixing Properties of a Microfluidic Device" by Daniel Kress , ChemE 499 Report, June 4, 2007.

VII. Appendix

$\rho = 1000\ kg/m^3$

$\eta = .001\ Pa\ s$

$D = 10^{-9}\ m^2/s$

X=200 micrometers

<v>=.005 m/s

Sample Calculation:

$p' = p/(\_ * v^2)$

p'= 101.7 from boundary integration on Incompressible Navier-Stokes solution at 2.5=z

$p = 101.7 * 1000\ kg/m^3 * (.005\ m/s)^2$

=2.54 Pa